Polymer 51 (2010) 3744–3752

Contents lists available at ScienceDirect

Polymer

journal homepage: www.elsevier.com/locate/polymer

Elongational creep experiments – A new method for investigations of morphology development in polymer blends

Zdeněk Starý*, Florian Machui, Helmut Münstedt

Institute of Polymer Materials, Friedrich-Alexander-University Erlangen-Nuremberg, Martensstr. 7, 91058 Erlangen, Germany

ARTICLE INFO

Article history:
Received 29 January 2010
Received in revised form
4 June 2010
Accepted 6 June 2010
Available online 12 June 2010

Keywords:
Blends
Morphology
Uniaxial elongation

ABSTRACT

This work is focused on the changes of phase structure in polystyrene/polyethylene blends with up to 15 wt.% of dispersed phase during elongational experiments in creep. In the first part, features of the experiments at constant stress with a special attention to morphology development in polymer blends are discussed. In the second part of the paper the deformation behavior of the dispersed droplets in dependence on applied stress and total strain is studied. It was found that with increasing the initial particle size the formation of homogeneously deformed long fibrils is preferred during the elongation. A maximum deformability of the droplets was observed, which cannot be increased by applying higher stresses, although the affine deformation of the droplets was not reached.

1. Introduction

The understanding and control of the blend morphology development in mixing equipments where two or more immiscible polymers are melt blended is a long-lasting dream of researchers in the field of polymer processing. In immiscible polymer blends, as typical example of heterogeneous systems, the inner microscopic phase structure of the material has a direct impact on macroscopic end-use properties. Therefore, controlling the morphology of these systems during processing can lead to materials with balanced mechanical and/or barrier properties tailored for particular applications.

The final phase structure of the blend is a result of the competition between droplet breakup and coalescence and besides the properties of the pure components it is markedly influenced by the processing conditions [1]. In the usual mixing devices, such as internal mixers or extruders, material is exposed to complex flow field containing both shear and elongational components. There are plenty of works trying to describe and model these complex flows, for example [2,3] and references in there. Besides that, a lot of valuable experimental studies like [4–6] and many others were performed in order to investigate the morphology development directly during the mixing. However, the deformation behavior of the droplets dispersed in the matrix is still not fully understood even for pure shear or elongational flow.

Basic theories of droplet deformation postulated by Taylor [7] and Cox [8] were derived for Newtonian liquids neglecting hydrodynamic interactions between neighboring droplets and they are valid only in the range of small deformations. Not surprisingly, deviations were reported for real polymer blends with viscoelastic properties [9–11] or higher amounts of dispersed phase [12]. Nevertheless, these theories using capillary number and viscosity ratio as main parameters are still a corner-stone for a qualitative prediction of morphology development in polymer blends. Taylor's theory enables a quantitative determination of droplet shape in two limiting cases: a) at low capillary numbers when a drop reaches its equilibrium deformation; b) at very high capillary numbers when the effect of interfacial tension can be neglected and an affine deformation of the particles occurs (see Delaby et al. [13] for details). In the region of moderate capillary numbers when hydrodynamic and interfacial stresses contest for the final droplet shape and breakup can occur, no quantitative description of droplet deformation is available, to our knowledge, even for Newtonian fluids.

Although the importance of elongational flow in processing of polymer blends is widely recognized, there are not many papers concerned with this topic. As already mentioned above, the basic works of Grace [14] or Janssen [15] investigating the influence of viscosity ratio on droplet deformation were performed on Newtonian systems using a four roller apparatus or an opposed jets device for generating planar elongational flow. Although the validation of their famous curve depicting the dependence of critical capillary number on viscosity ratio was not performed for uniaxial elongation till now, it is commonly used for that purpose.

* Corresponding author. Tel.: +49 (0) 9131 85 27748; fax: +49 (0) 9131 85 28321.
E-mail address: zdenek.stary@ww.uni-erlangen.de (Z. Starý).

0032-3861/$ – see front matter © 2010 Elsevier Ltd. All rights reserved.
doi:10.1016/j.polymer.2010.06.017

The influence of the viscosity ratio on droplet deformation in non-Newtonian systems was studied by Delaby et al. [13,16]. The deformation was studied at very low or very high capillary numbers, i.e. under conditions where droplet breakup during elongation is not possible. It was found that the droplets deform less than the macroscopic sample if they are more viscous than the matrix and vice versa which is in agreement with Taylor's [7] and Cox' theories [8]. The impact of the elasticity of the components on droplet behavior was also investigated [9–11]. It was observed that droplet deformation increases with increasing elasticity of the matrix and decreases with increasing elasticity of the droplet.

For the determination of capillary number and its critical value in elongation, the shear viscosities are usually used following the procedure described in [13]. However, this can lead to pronounced discrepancies in systems with distinct non-linear effects such as strain hardening. The direct use of elongational viscosities in capillary number model was first performed by Heindl [17] followed by Stary [18].

All the studies mentioned above were performed using stressing experiments, i.e. experiments at constant strain rate. Because of the transient nature of the elongational viscosity of viscoelastic polymer melts, the capillary number as a basic parameter determining the droplet deformation is not constant during the elongation. Therefore, in this case the predictions made by Taylor's theory can be used only as a rough approximation. Again, this becomes even more important in systems displaying strain hardening behavior. On the other hand, the experiments at constant stress offer the possibility to deform the droplets under defined conditions at constant capillary number regardless of the non-stationary state. Elongational creep experiments were firstly described more than 30 years ago by Laun and Münstedt [19]. However, in spite of their advantages they are only rarely used for the characterization of polymer melts [20] or for the investigations of morphology development in polymer blends [21]. That is mainly because of the high technical demands on the rheometer control unit. Recently, the development of a new device able to perform creep experiments was reported by Maia et al. [22] but a validation of reliability and accuracy of the measurements is needed.

This work is concerned with phase structure changes in immiscible polymer blends during elongational creep experiments. The first part is focused on a detailed description of features of the experiments at constant stress with a special attention on the morphology development in polymer blends. In the second part of the paper the deformation behavior of the dispersed droplets in dependence on the applied stress and total strain is studied. The experimental findings are compared with the predictions of the capillary number model using the directly obtained elongational data only.

2. Experimental

2.1. Materials and specimen preparation

Polystyrene (PS), type 158 K with a density of 1.050 g cm^{-3} (20 °C) was supplied by BASF. The linear low-density polyethylene (LLDPE), type LL 1001 XV with a density of 0.919 g cm^{-3} (20 °C) provided by ExxonMobil Chemical, is a copolymer of ethene and 1-butene.

The blends with polystyrene as the matrix and 5, 10 or 15 wt.% of LLDPE as a dispersed phase were prepared in the twin-screw extruder Leistritz LSM 34GL ($L/D = 32$) at 190 °C and a screw speed of 20 rpm.

For the extensional experiments cylindrical specimens with a length of 25 mm and a diameter of 5 mm were used. At first a strand was extruded through a capillary at 190 °C and an apparent shear stress of 43.7 kPa. The strand was extruded into an ethanol–water mixture with adapted density in order to ensure a homogeneous strand diameter along the axes of the extrusion. After extrusion the strand was annealed in a silicone oil bath at 150 °C for 30 min. This step ensures a complete relaxation of the stresses accumulated in the sample. Then the strand was cut into 25 mm long pieces. Surface was etched by air plasma to increase the surface energy which is necessary to reliably glue the samples to aluminium clamps using the two-component epoxy resin Technicoll 8266/67.

2.2. Elongational creep experiments

The device used for the elongational measurements in this study was the Münstedt elongational rheometer. Its detailed description can be found elsewhere [23]. In this device the specimen is immersed in a silicone oil bath in order to suppress inhomogeneous deformation caused by a density mismatch and elongated in vertical direction. A unique feature of the Münstedt elongational rheometer is that it can perform also the experiments at constant stress besides the usual experiments at constant strain rate. If we assume a constant volume of the specimen during the elongation, the following relation (Eq. (1)) is fulfilled:

$$\sigma = \frac{F}{A_0} = \frac{F(t)}{A(t)} = \frac{F(t)\cdot L(t)}{A_0 \cdot L_0} \tag{1}$$

where σ is the desired imposed stress, F the tensile force, A the cross-section of the specimen perpendicular to the deformation axis, L the length of the specimen. The subscript 0 stands for the dimensions of the specimen at the beginning of the experiment. Because of the continual decrease of the specimen's cross-section during the experiment, the rheometer is equipped with an advanced control unit which set the actual tensile force F to the value corresponding to the control condition $F(t)\cdot L(t) = \text{const}$ (Eq. (1)). Then the actual stress imposed on the specimen is kept constant during the whole experiment under the assumption of an ideally homogeneous deformation.

The elongational experiments were performed at 170 °C on cylindrical specimens the preparation of which is described above. The specimens were deformed at stresses ranging from 1 to 50 KPa to the maximal Hencky strain ε_H of three. A typical example of the creep measurement is shown in Fig. 1. When the stationary state is reached, the time dependence of the Hencky strain becomes linear and the slope represents the value of the stationary strain rate $\dot{\varepsilon}_{stat}$ Then one can easily estimate the stationary elongational viscosity μ_{stat} as the ratio of the constant value of the applied stress σ and $\dot{\varepsilon}_{stat}$.

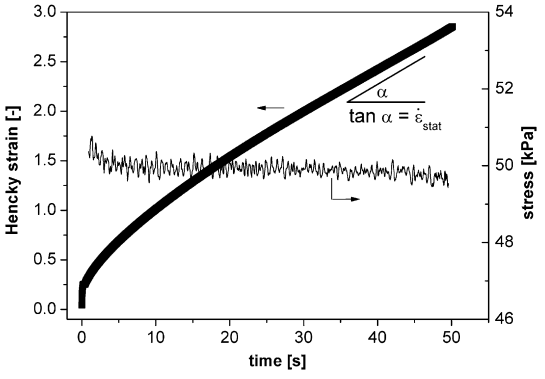

Fig. 1. Example of elongational creep experiment on the PS/LLDPE 95/5 blend at 170 °C and 50 kPa.

After the elongation the specimen is quickly removed from the oil bath of the rheometer and immersed in liquid nitrogen. The time needed to cool down the specimen below the glass transition temperature of polystyrene matrix where morphology changes cannot occur anymore is typically around 7 s. According to literature [17,21,24], this time is short with respect to the shape relaxation of droplets. This was proved also experimentally (see Appendix) and, therefore, the phase structure observed is very close to the real morphology of the sample.

2.3. Scanning electron microscopy

The morphology of the elongated specimens was studied by means of scanning electron microscopy (SEM). The specimens were fractured in liquid nitrogen in order to avoid plastic deformations of the material in the direction parallel to the deformation axis. The broken surfaces were then coated by a thin layer of palladium using a Sputter Coater S150B (Edwards). All micrographs were taken by the electron microscope LEO 435 VP at an acceleration voltage of 10 kV using a secondary electron detector. Only the phase structures of the blends elongated to Hencky strains smaller than two were investigated. The highly elongated specimens ($\varepsilon_H > 2$) had insufficient diameter for the preparation of satisfactory lengthwise fractures.

The average diameters of the dispersed particles perpendicular to the tensile axis and their distributions were evaluated by means of an image analysis using the software Leica QWin. For every sample, around 800 particles from at least three different areas of the specimen were measured. The accuracy of image analysis was estimated as the size of one pixel in the micrographs. As the magnification of the micrographs used for image analysis was different for the PS/LLDPE 95/5 and for more concentrated systems, this value was 0.0125 μm and 0.025 μm, respectively.

3. Results and discussion

3.1. Benefits of the creep experiments

In this section the benefits of experiments at constant stress with a special attention on the morphology development in polymer blends are discussed.

The behavior of a liquid droplet dispersed in a liquid matrix under stress is usually described using two dimensionless parameters – capillary number *Ca* (determining the deformation of the dispersed droplets qualitatively) and viscosity ratio *p* [7]. Generally, the capillary number is the ratio of the hydrodynamic stress (σ) applied to the droplets which forces the drop to deform, and the interfacial stress ($2\cdot\Gamma_{12}/d$) which tends to preserve the spherical shape of the droplet in order to minimize its surface energy. In the case of elongational flow, *Ca* and *p* can be defined as:

$$Ca = \frac{\sigma\cdot d}{2\cdot\Gamma_{12}} = \frac{\mu_m\cdot\dot{\varepsilon}\cdot d}{2\cdot\Gamma_{12}} \tag{2}$$

$$p = \frac{\mu_d}{\mu_m} \tag{3}$$

where μ_m and μ_d are the elongational viscosities of the matrix and the dispersed phase, $\dot{\varepsilon}$ is the strain rate, d is the diameter of the particle and Γ_{12} is the interfacial tension. If the capillary number *Ca* overcomes its critical value Ca_{CR}, the dispersed droplet starts to deform continually and it can breakup at higher deformation.

The critical capillary number was found experimentally to be a function of the viscosity ratio *p* of the blends components [14,25] and for planar elongational flow it can be fitted by the following function [26]:

$$\log Ca_{CR} = -0.64853 - 0.02442\cdot\log p + 0.02221\cdot(\log p)^2 - \frac{0.00056}{\log p - 0.00645} \tag{4}$$

Therefore, a correct and accurate estimation of the viscosity ratio at given conditions of elongation is necessary for the prediction of droplets behavior using the capillary number model. Nevertheless, for an estimation of the viscosity ratio in elongation shear data from dynamical mechanical analysis are commonly used [13] with the assumption of a validity of the Cox-Merz rule. This approach assumes that for a generalized Newtonian fluid the viscosity is a function of the second invariant of the strain rate tensor *D* [27]:

$$\eta = f\left[\sqrt{2\cdot tr(D)^2}\right] \tag{5}$$

The term in brackets simplifies to the shear rate in shear or to $\sqrt{3}\cdot\dot{\varepsilon}$ in uniaxial elongation. Then the dynamic viscosities of the blend components at $\omega = \sqrt{3}\cdot\dot{\varepsilon}$ are used to determine the viscosity ratio. In this work the viscosity ratios were estimated using the values of the directly measured stationary elongational viscosities of the pure PS and LLDPE at given stress. Fig. 2 shows the stress dependence of μ_{stat} of the pure components compared with the classical shear viscosity curves. One can see in Fig. 2a that the viscosity μ_{stat} of PS matrix increases slightly with the applied stress indicating a weak strain hardening of the material used. Contrary to that, the

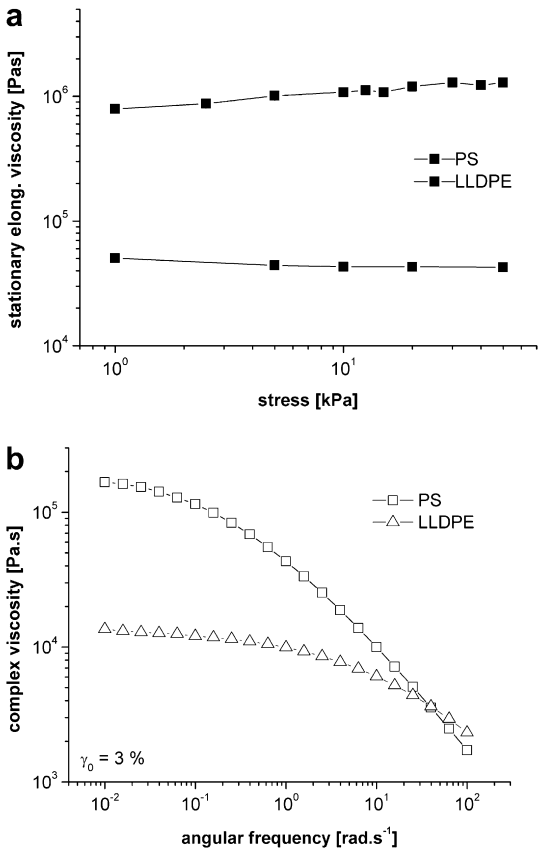

Fig. 2. Flow behavior of PS and LLDPE at 170 °C: a) stationary elongational viscosity as a function of applied stress; b) magnitude of the complex shear viscosity as a function of the angular frequency.

viscosity of the LLDPE is constant in the whole range of the stresses investigated. The values of the viscosity ratios for chosen stresses determined by both methods, i.e. using shear data or directly stationary elongational viscosities, are summarized in Table 1.

It is obvious that the viscosity ratio $p_E = \mu_{LLDPE,stat}/\mu_{PS,stat}$ which is based on elongational data decreases with increasing stress because of the slight strain hardening behavior of the PS matrix. On the other hand, the viscosity ratio p_S based on shear data displays a rather constant value with a tendency to a slight increase at higher stresses. Despite of the fact that the dependence of Ca_{CR} on p is not very steep, this discrepancy can lead to the wrong estimation of Ca_{CR} and consequently to the failure of the capillary number model. This becomes even more evident in the cases of polymer systems with pronounced non-linear effects such as strain hardening. Therefore, in the following parts only the viscosity ratios p_E will be used for an estimation of Ca_{CR}.

The advantage of creep experiments in comparison to experiments at constant strain rate is that the stationary state of deformation is reached much faster, i.e. at smaller total elongations. This allows one to determine the stationary elongational viscosity even in the cases if the stationary state is not attainable in stressing experiments at all [20]. This feature is illustrated in Fig. 3 on a PS/LLDPE 95/5 blend at 170 °C. The strain rate of 0.0424 s^{-1} used in the stressing experiment was chosen in a way that it corresponds to the stationary strain rate in the creep experiment at 50 kPa. One can clearly see that the stationary state is not reached during the whole stressing experiment, i.e. the transient elongational viscosity increases monotonously approaching the steady-state viscosity at longer experimental times. On the other hand, in creep experiment the stationary state is observed after approximately 30 s which corresponds to total a Hencky strain of two (cf. Fig. 1) and stationary elongational viscosity can be determined. With decreasing stress applied the attainment of the stationary state is shifted to even smaller Hencky strains. For example, for the stress of 10 kPa the stationary state is reached already at $\varepsilon_H = 0.5$.

A crucial difference between creep and stressing experiments appears if one looks at the definition of the capillary number more closely (cf. Eq. (2)). It is clear that during the stressing experiment the value of Ca is not constant unless the stationary state is reached. This becomes a serious problem in case of strain hardening materials as discussed above. Contrary to that, during the creep experiment the value of Ca is fixed at all times regardless of the stationarity of deformation because the hydrodynamic stress $\sigma = \mu_m \cdot \dot{\varepsilon}$ imposed on the specimen is kept constant. Moreover, the use of the creep mode allows one to avoid the dilemma whether to take into computation the viscosity of the matrix or the viscosity of the blend as proposed by Caserta et al. [12] for concentrated systems where hydrodynamic interactions of the droplets cannot be excluded. The comparison of the time dependence of Ca in a creep and a corresponding stressing experiment is shown in Fig. 4. Because during the stressing experiment the stationary state was not reached at all, the value of Ca increases continuously. Therefore, the prediction of the droplet behavior based on a comparison of Ca and its critical value Ca_{CR} during the non-stationary stressing experiment can be used only as a rough hint.

Table 1
Comparison of viscosity ratios directly determined from elongational measurements with those obtained from corresponding shear data.

σ (kPa)	$\dot{\varepsilon}_{stat}$ (s^{-1})	ω (rad s^{-1})	p_E (−)	p_S (−)
1	0.001	0.002	0.064	–
5	0.006	0.010	0.043	0.081
10	0.010	0.017	0.040	0.081
20	0.018	0.031	0.036	0.084
50	0.043	0.074	0.033	0.100

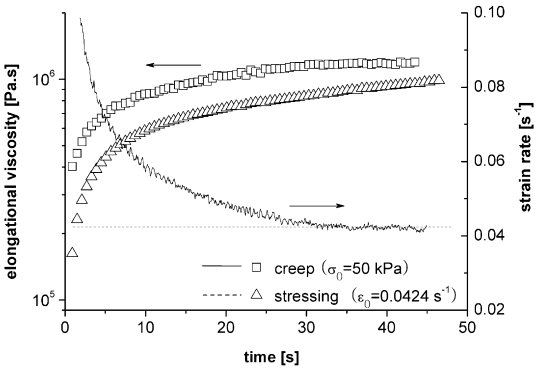

Fig. 3. Comparison of a creep experiment at 50 kPa and a corresponding stressing experiment at 0.0424 s^{-1} for the PS/LLDPE 95/5 blend at 170 °C.

Contrary to that, in the creep experiment the Ca is constant during the whole deformation.

Generally, elongational experiments at constant stress make it possible to perform morphology development investigations under defined conditions, i.e. at constant Ca. Furthermore, it enables to use the capillary numbers without the need of shear data which can lead to discrepancies between theoretical predictions and experimental results.

3.2. Morphology development

The second part of the paper is concerned with the deformation behavior of the droplets in PS/LLDPE blends with 5, 10 and 15 wt.% of the dispersed phase during elongation at constant stress.

One of the assumptions of the use of Ca for prediction of particle deformation is an isotropic initial morphology of the blend. Fig. 5 shows the phase structure of the blends studied directly prior to a deformation in the elongational rheometer. One can observe typical features of immiscible polymer systems such as sharp and smooth interfaces, holes remained by particles fallen out of the matrix due to a weak interfacial adhesion or very broad distribution of dispersed particle sizes. Obviously, the average droplet diameter increases with the growing amount of the dispersed phase. This finding is in agreement with the existing theoretical considerations dealing with morphology development [28] and it is explained as a consequence of a more pronounced flow induced coalescence during mixing. In our case the average particle size rises from 0.61 μm for the blend with 5 wt.% of LLDPE (Fig. 5a) to 0.90 μm and 1.39 μm in the cases of 10 and 15 wt.% of dispersed phase, respectively (Fig. 5b and c).

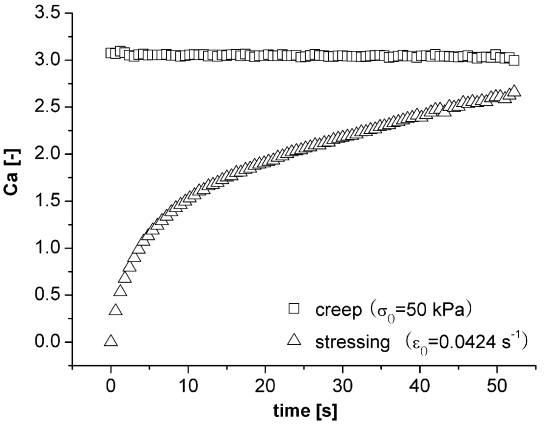

Fig. 4. Evolution of capillary number during a creep experiment at 50 kPa and a corresponding stressing experiment at 0.0424 s^{-1} for the PS/LLDPE 95/5 blend at 170 °C.

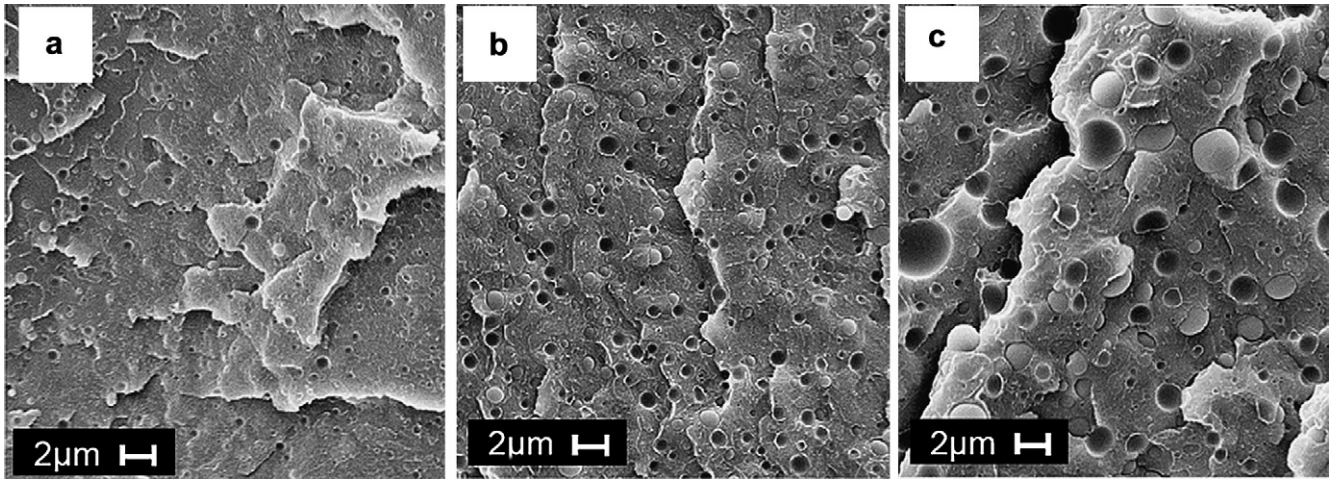

Fig. 5. Phase structures of PS/LLDE blends prior to elongation: a) 95/5; b) 90/10; c) 85/15.

The original phase structures shown in Fig. 5 were exposed to stresses in the range of 1–50 kPa. The capillary number is constant during creep experiments and increases linearly with the stress applied as described above. Fig. 6a shows the stress dependence for the PS/LLDPE blend with 5 wt.% of dispersed phase. With respect to the critical capillary number Ca_{CR}, determined using stationary elongational viscosities and Eq. (4) as described above, one can distinguish three main deformation regions. Because of the direct use of elongational viscosities in the definition of capillary number, the values of Ca_{CR} calculated from Eq. (4) were multiplied by a factor of 3 according to Trouton's law [14].

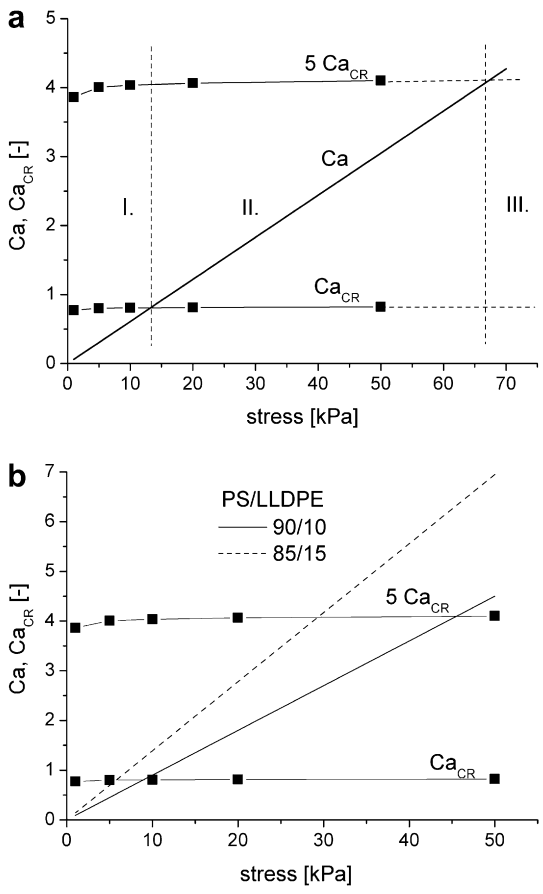

Fig. 6. Capillary numbers and the critical values as a function of applied stress for elongational experiments in creep: a) PS/LLDPE 95/5; b) PS/LLDPE 90/10 and PS/LLDPE 85/15.

At low capillary numbers (region I), where the critical value is not reached, the particles are not deformed at all or they are only slightly deformed to stable rotational ellipsoids. In PS/LLDPE 95/5 this region corresponds to stresses lower than 13 kPa. Increasing the hydrodynamic stress, Ca_{CR} is exceeded and the particles should deform continually and at high enough deformations they can breakup into smaller particles (region II). At very high capillary numbers a third deformation region was experimentally found [15,29] where an affine deformation of the particles occurs and highly elongated fibrils are formed (region III). These fibrils are supposed to be stable during deformation and to breakup after cessation of the flow. In elongation the value of Ca separating the second and third region from each other was found to be the fivefold of Ca_{CR} [15,29] which in our case comes up to the stress of about 65 kPa. In the systems containing 10 or 15 wt.% of dispersed phase the stress dependence of the capillary number becomes steeper because of the increasing diameter of the initial particles (Fig. 6b). Accordingly to that fact, the stresses at which Ca reaches Ca_{CR} and 5 Ca_{CR} are shifted to lower values. It is worth noting again, that main assumption of these predictions is a Newtonian behavior of the blend components, which is not the case, however, for the materials used in this study. Therefore, discrepancies between these predictions and experimentally found results would not be surprising.

The morphologies of the PS/LLDPE 95/5 elongated to a Hencky strain of two at different stresses were investigated by SEM and they are displayed in Fig. 7. One can see that in the case of stresses of 10 kPa and lower (region I, Fig. 7a and b) the dispersed particles are only slightly deformed which is in agreement with predictions of the capillary number model (Fig. 6a). Exceeding the critical value of Ca, pronounced deformation of particles should be observed (region II). At stresses of 15 and 20 kPa (Fig. 7c and d) a mix of phase structures is present in the material. Small almost non-deformed particles, elongated drops and even a few highly stretched particles are distinguishable in the micrographs (Fig. 7c and d). This diversity can be explained as a result of breakup processes occurring during the deformation at moderate values of capillary number ($Ca > Ca_{CR}$). If the elongated droplet breaks up during the flow, the newly formed smaller particles can undergo further deformation or they can be stable in the flow, when the

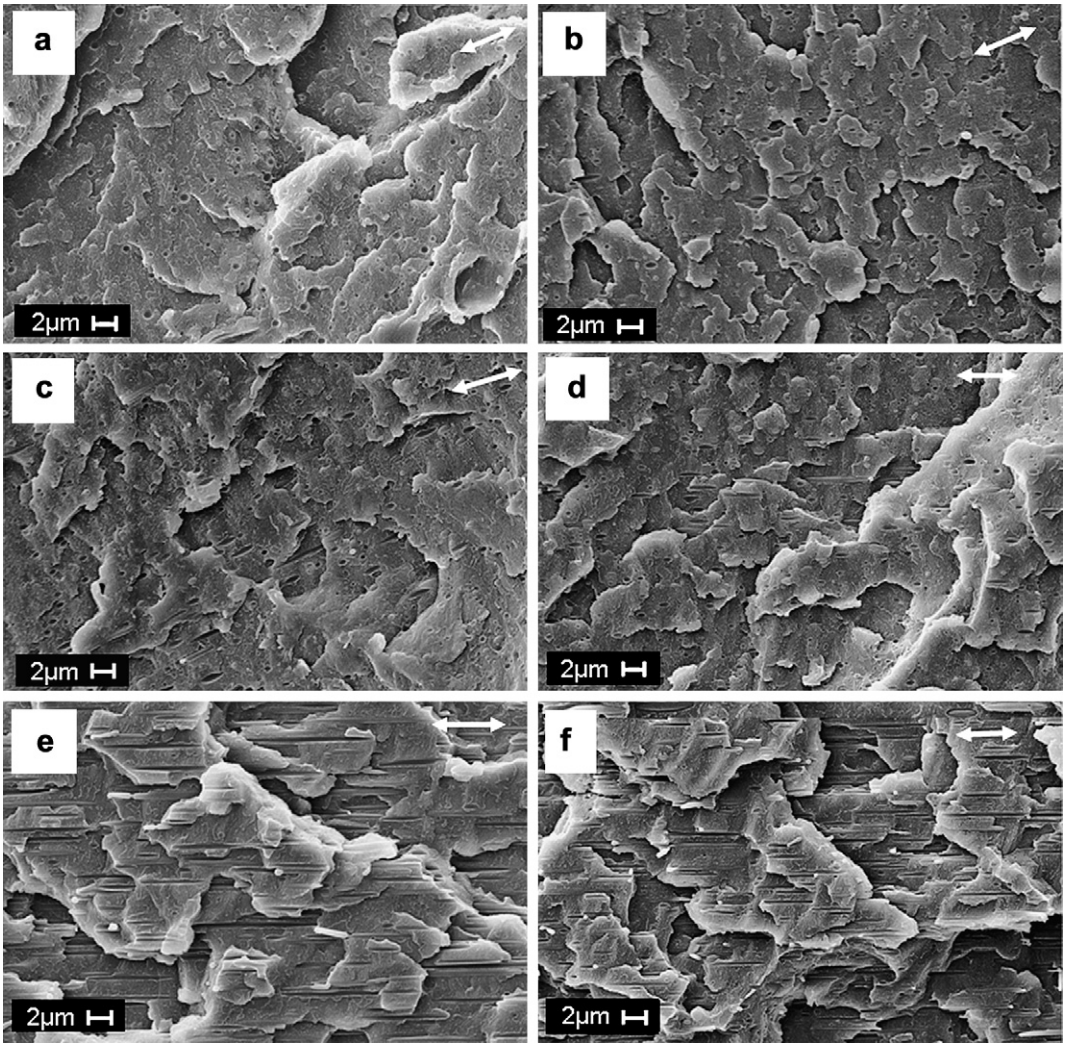

Fig. 7. Morphologies of the PS/LLDPE 95/5 blend after deformation to $\varepsilon_H = 2$ at 170 °C and constant stress of: a) 2.5 kPa; b) 10 kPa; c) 15 kPa; d) 20 kPa; e) 30 kPa; f) 40 kPa.

interfacial stress is high enough. Then the differently deformed particles can be detected in the material. When the stress imposed on the particles increases to 30 kPa and more, only highly elongated fibrils are detected in the material (Fig. 7e and f). However, this behavior, i.e. the formation of stable fibrils, is predicted by the capillary number model only at stresses higher than 65 kPa (region III, Fig. 6a).

This discrepancy becomes even more pronounced in the systems with higher amounts of the dispersed phase, i.e. in the systems containing bigger particles. Fig. 8 shows morphologies of the PS/LLDPE 90/10 and 85/15 blends deformed at 2.5 and 5 kPa to a Hencky strain of two. At the low stress of 1 kPa the spherical shape of the particles is approximately preserved for both materials (not shown). At 2.5 kPa the particles in PS/LLDPE 90/10 are only very slightly deformed (Fig. 8a) which corresponds to the theoretical prediction, because the critical capillary number is not exceeded (Fig. 6b). Increasing the stress to 5 kPa, the droplets become highly stretched and a fibrillar phase structure is formed (Fig. 8b), although the value of Ca_{CR} is not reached. At all higher stresses in the range from 10 to 50 kPa, the particles behave qualitatively in the same way. They are elongated to long fibrils without any signs of droplet breakup. Very similar results are found for the blend containing 15 wt.% of dispersed phase. In this case the deformation at 2.5 kPa already leads to the formation of markedly elongated droplets (Fig. 8c). At all stresses of 5 kPa (Fig. 8d) and higher the presence of highly stretched fibrils was observed.

In these systems with the higher amount of dispersed phase the mixed morphology explained as a consequence of droplet breakups was not detected at all. This can be explained as follows. The breakup of a deformed droplet is preceded by the formation of a neck. The driving force of this neck formation is the interfacial stress which tries to minimize the surface energy. According to the definition, the interfacial stress is inversely proportional to the diameter of the particle. Hence, the interfacial stress is smaller in the case of larger particles and it is not strong enough to induce the inhomogeneous deformation of the droplet (neck formation) which can further lead to breakups. Instead of that, only the formation of long homogeneously deformed fibrils is observed up to a Hencky strain of two. Moreover, at higher concentrations of the dispersed phase the flow induced coalescence of the particles cannot be excluded. This would lead to a further increase in droplet size and consequently to the suppression of droplet breakup. This phenomenon, i.e. a more pronounced fibril formation by increasing the amount of dispersed phase, was found also in complex flow fields during extrusion [30].

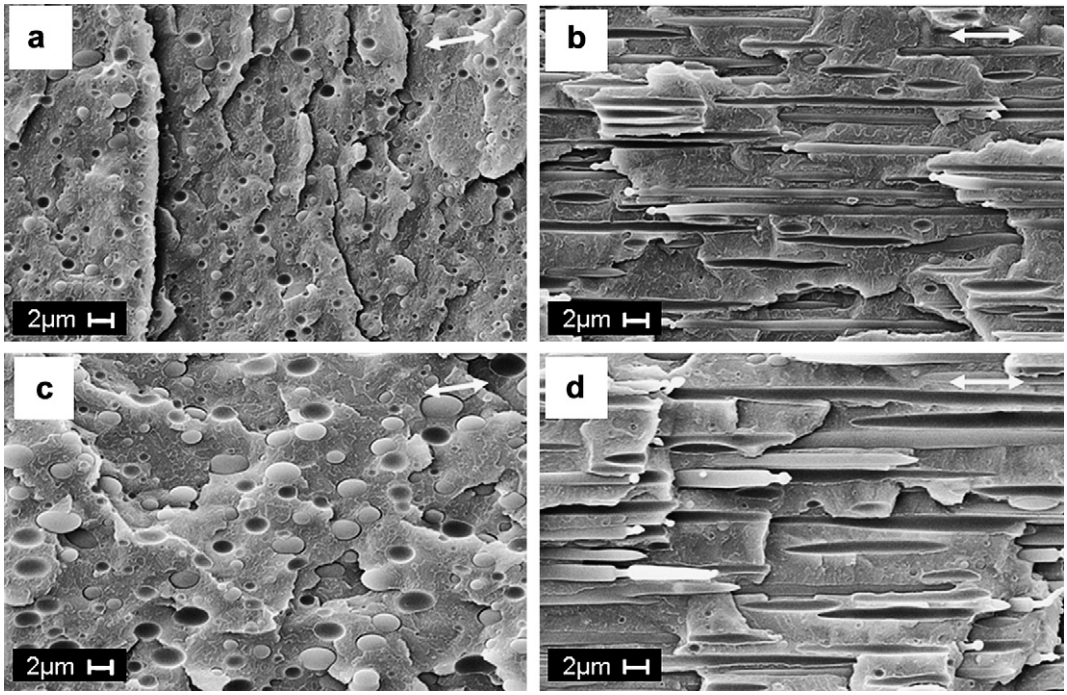

Fig. 8. Morphologies of PS/LLDPE blends with higher amounts of the dispersed phase after deformation to $\varepsilon_H = 2$ at 170 °C and constant stress: a) PS/LLDPE 90/10, 2.5 kPa; b) PS/LLDPE 90/10, 5 kPa; c) PS/LLDPE 85/15, 2.5 kPa; d) PS/LLDPE 85/15, 5 kPa.

Using the image analysis of the SEM micrographs one can obtain the particle diameters perpendicular to the tensile axis at a Hencky strain of two for different blend compositions as a function of the applied stress. Such a quantitative evaluation of the morphologies can be seen in Fig. 9. For a better comparison of the different blends the real average diameters of the deformed particles are divided by the average diameter of the droplets prior to elongation. Some interesting effects can be derived from this plot.

First, the particle deformation is a function of the total amount of the dispersed phase, i.e. the initial particle size. Larger particles are deformed more than the smaller ones in the whole range of stresses studied because of the decreasing role of the interfacial stress ($2\cdot\Gamma_{12}/d$) which counteracts the deformation. Second, in all systems a constant value of particle diameter was observed at high stresses when $Ca >> Ca_{CR}$ and the fibril morphology is formed.

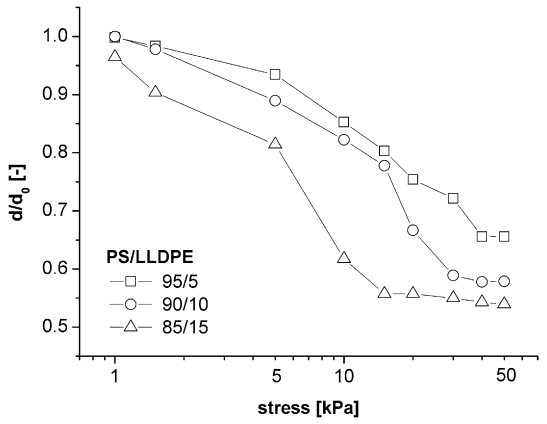

Fig. 9. Normalized particle diameters of PS/LLDPE blends after elongational creep experiments to $\varepsilon_H = 2$ at 170 °C as a function of stress applied (d – the average particle diameter perpendicular to the flow direction obtained under definite conditions, d_0 – initial average particle diameter).

Such a behavior is expected if the deformation of droplets is affine, in other words if the droplet deformation is the same as the total deformation of the specimen. However, this is not the case here. The affine deformation of the droplets at a Hencky strain of two should result in the value of $d/d_0 = \exp(-\varepsilon_H/2) = 0.37$. This value was not reached in any of the experiments performed. Moreover, the maximum deformation of the droplets, i.e. the lowest d/d_0, is also a function of the initial particle size. Increasing the original droplet diameter, the maximum droplet deformability raises, but the affine deformation was not reached. Again, the decreasing role of the interfacial stress in blends with larger particles can be claimed as a reason for this effect. The beginning of the plateau is shifted to lower stresses as the initial droplet size increases. If one compares the values of stresses at which the particles are not deformed further with values of the capillary numbers (Fig. 6), it is obvious that the onset of the plateau corresponds to Ca/Ca_{CR} of approximately three for all systems. The effect known as a slip at the interface [31,32] could be one of the reasons for maximum deformability of the droplets. The slip at the interface is observed in the systems with no or weak interactions between the phases which is the case of immiscible polymer blends. This effect occurs mainly at high stresses at which the stress is not fully transferred from the matrix to the dispersed phase [33].

The morphology development during the elongation, i.e. not only the final stage at a Hencky strain of two as in the foregoing paragraphs, was studied for the blend with 5 wt.% of LLDPE. The stresses used in this study were chosen in order to describe the phase structure changes in all three deformation regions (Fig. 6a). The average particle diameters perpendicular to the direction of deformation as a function of the total elongation are displayed in Fig. 10.

At the stress of 2.5 kPa where $Ca < Ca_{CR}$ (region I) and the particles are almost non-deformed (Fig. 7a) the average particle size stays practically constant in the whole range of deformation. A more interesting behavior can be observed in region II (stresses of 10, 15 and 20 kPa) where $Ca > Ca_{CR}$. Here after an initial decrease

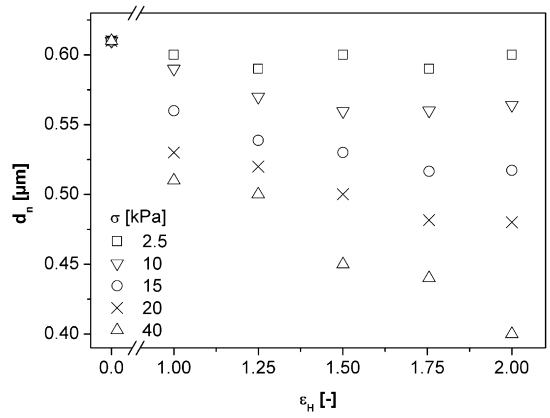

Fig. 10. Average particle diameter (perpendicular to the flow direction) as a function of Hencky strain during elongational creep experiments of PS/LLDPE 95/5 at 170 °C and different stresses.

the average particle diameter levels off and the finally reached value decreases with increasing hydrodynamic stress (Fig. 10). As the variety of phase structures can be found in these specimens (see Fig. 7c and d), it is highly probable that in this region the breakups of the deformed droplets take place. Breakups lead to the formation of smaller particles which can be stable in the flow or they can undergo further deformations and possible breakups. The higher the stress applied, the smaller are the particles being able to survive in the flow without deformation. It is worth noting that a breakup of elongated droplet leads to an increase of the lateral diameter whereas a deformation results in the opposite effect. Therefore, the constant value of the average particle lateral dimension does not mean that the morphology is not changing. It is possible that in the range of strains at which the lateral diameter is constant, there is a kind of dynamic equilibrium between deformation and breakup of the particles.

At stresses at which the fibrillar morphology is formed (region III, Fig. 7f) the average lateral diameter of the particles decreases during the whole deformation and this decrease is more pronounced than in the cases where breakups are supposed to occur. That means that the particles are continually elongated and the droplet breakup is markedly suppressed. These findings are in agreement with the capillary number model which predicts a formation of fibrils stable in the flow for $Ca >> Ca_{CR}$ as the effect of interfacial stress can be neglected in this region.

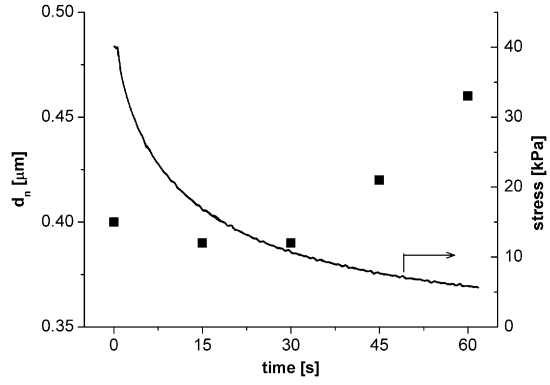

Fig. 11. Average particle diameter (perpendicular to the flow direction) as a function of time after the elongation of the PS/LLDPE 95/5 blend (170 °C, 40 kPa, $\varepsilon_H = 2$) and the relaxation of the stress.

4. Conclusion and outlook

Elongational creep experiments as a new method for investigations of morphology development in polymer blends are described in this paper. Despite of numerous advantages, creep experiments have not been used at all for such investigations till now. Contrary to usually conducted experiments at constant strain rate, elongational creep experiments allow one to perform the deformation of dispersed droplets under defined conditions. In creep, the stress imposed on the sample is constant and, therefore, the capillary number determining the deformation of the dispersed droplets is also constant during the whole experiment and it is directly proportional to the stress applied. Another advantage is that in creep experiments the stationary state is reached at smaller total elongations than in experiments with constant strain rate and so one can obtain the steady elongational viscosity easily for a number of polymer materials. Moreover, no additional shear data are needed for a prediction of the morphology development in elongation using the capillary number.

From the elongational creep experiments it was found that with increasing the initial particle size the formation of homogeneously deformed long fibrils is preferred instead of droplet breakups. This is explained by the decreasing role of the interfacial stress with increasing size of the deformed droplets. In such cases the interfacial tension is not strong enough to induce a neck formation followed by a droplet breakup during the flow. Furthermore, a maximum deformability of the droplets in the blends elongated to Hencky strain of two was observed, which cannot be increased by applying higher stresses, although the affine deformation of the droplets was not reached. This behavior was observed at stresses corresponding to $Ca/Ca_{CR} > 3$. The slip at the interface could be one of the reasons for this phenomenon. This maximum deformability was found to increase with the initial particle size.

From the method of elongational creep experiments introduced in this paper it is obvious that measurements of droplet deformation at constant capillary numbers can be easily performed even for polymer blends with non-Newtonian behavior. Hence, creep experiments could be used to extend the pioneering works of Grace [14] and Janssen [15] on Newtonian materials for non-Newtonian systems which are of a widespread interest. Their results are commonly used for a prediction of the droplet behavior in elongational flow in spite of the fact, that they were performed on Newtonian systems and in planar elongation, only. Investigations on the morphology development in non-Newtonian polymer blends applying the technique described before are time-consuming, of course, but they would lead to a more reliable base for an assessment of the particle deformation in blends of engineering polymers.

Acknowledgement

The authors are grateful to the German Research Foundation (grant Nr. STA 1096/1-1) for the financial support and also want to thank Mr. A. Kirchberger for inspiring discussions.

Appendix. Freezing-in the blend morphology

To verify the assumption that the phase structure of the specimens removed from the rheometer, quenched in liquid nitrogen, and finally observed by SEM is very close to the real blend morphology imposed by the elongation, the following experiments were performed. The PS/LLDPE 95/5 blend was elongated at a temperature of 170 °C and a stress of 40 kPa to the total Hencky strain of two. These conditions lead to the formation of highly elongated PE particles (Fig. 7f). Considering the high surface energy of these fibrils, such morphology is unstable and it is inclinable to the changes in the time after the cessation of the flow and before

the specimen is frozen in. To investigate this behavior, the deformed specimens were kept inside the rheometer in the elongated state for variable time periods up to 60 s after elongation. Then they were removed from the rheometer and immersed in liquid nitrogen. The results of the image analysis of the micrographs together with the dependence of the stress stored in the elongated specimen on the time after cessation of the flow are shown in Fig. 11.

It can be seen that no change in the particle lateral diameter was observed during the first 30 s after cessation of the flow. In this time period the stress in the specimen decreases due to the relaxation of polymer chains from the initial value of 40 kPa to approximately 10 kPa. In this region of stresses the capillary number is larger than its critical value (cf. Fig. 6a) which means that the stress is still high enough to hold the dispersed particles in the elongated state. After 30 s the particle lateral diameter starts to increase which can be associated either with a retraction of the elongated droplets or with their breakup. With continuing relaxation of polymer chains the hydrodynamic stress stored in the specimen further decreases and the interfacial stress can induce the above mentioned changes in the blend morphology. As the time needed to remove the specimen from the rheometer and cool it below the glass temperature of the PS matrix is about 7 s, we can say that within the accuracy of the image analysis the phase structure observed by SEM is identical with the real blend morphology induced by the elongation.

References

[1] Favis BD. Factors influencing the morphology of immiscible polymer blends in melt processing. In: Paul DR, Bucknall CB, editors. Polymer blends. Formulation, vol. 1. New York: Wiley; 2000. p. 501–39.
[2] Kajiwara T, Nagashima Y, Nakano Y, Funatsu K. Polym Eng Sci 1996;36(16):2142–52.
[3] Braun A, Dressler M, Windhab EJ. J Non-Newtonian Fluid Mech 2008;149(1–3):93–103.
[4] Lee JK, Han CD. Polymer 1999;40(23):6277–96.
[5] Lee JK, Han CD. Polymer 2000;41(5):99–1815.
[6] Li H, Sundararaj U. Macromol Chem Phys 2009;210(10):852–63.
[7] Taylor GI. Proc Roy Soc 1932;138:41–8.
[8] Cox RG. J Fluid Mech 1969;37:601–23.
[9] Leal LG, Milliken WJ. J Non-Newtonian Fluid Mech 1991;40:355–79.
[10] Mighri F, Ajji A, Carreau PJ. J Rheol 1997;41:421–36.
[11] Vinckier I, Moldenaers P, Mewis J. J Rheol 1997;41:705–18.
[12] Caserta S, Reynaud S, Simeone M, Guido S. J Rheol 2007;51:761–74.
[13] Delaby I, Ernst B, Germain Y, Muller R. J Rheol 1994;38(6):1705–20.
[14] Grace HP. Chem Eng Commun 1982;14:225–77.
[15] Janssen JMH. Dynamics of liquid–liquid mixing. Ph.D. Thesis. Eindhoven University of Technology; 1993
[16] Delaby I, Ernst B, Froelich D, Muller R. Polym Eng Sci 1996;36(12):1627–35.
[17] Heindl M, Sommer MK, Münstedt H. Rheol Acta 2004;44:55–70.
[18] Stary Z, Münstedt H. J Polym Sci Part B Polym Phys 2008;46:16–27.
[19] Laun HM, Münstedt H. Rheol Acta 1976;15:517–24.
[20] Münstedt H, Auhl D. J Non-Newtonian Fluid Mech 2005;128:62–9.
[21] Kirchberger A, Münstedt H. J Rheol 2010;54(3):687–704.
[22] Maia JM, Andrade RJ, Covas JA, Laeuger J. AIP Conf Proc 2008;1027:1111–3.
[23] Münstedt H, Kurzbeck S, Egersdörfer L. Rheol Acta 1998;37:21–9.
[24] Mechbal N, Bousmina M. Rheol Acta 2004;43:119–26.
[25] Bruijn RA. Deformation and breakup of drops in simple shear flows. PhD Thesis. EindhovenUniversity of Technology; 1989.
[26] Utracki LA, Shi ZH. Polym Eng Sci 1992;32(24):1824–33.
[27] Jones DM, Walters K, Williams PR. Rheol Acta 1987;26:20–30.
[28] Fortelny I. Theoretical aspects of phase morphology development. In: Harrats C, Thomas S, Groeninckx G, editors. Micro- and nanostructured multiphase polymer blend systems: phase morphology and interfaces. Boca Raton: Taylor and Francis; 2006. p. 43–90.
[29] Elemans PHM, Bos HL, Janssen JMH, Meijer HEH. Chem Eng Sci 1993;48:267–76.
[30] Chapleau N, Favis BD. J Mater Sci 1995;30:142–50.
[31] Helfand E, Tagami Y. J Polym Sci Part B Polym Lett 1971;9:741–6.
[32] Zhao R, Macosko CW. J Rheol 2002;46(1):145–67.
[33] Bousmina M, Palierne JF, Utracki LA. Polym Eng Sci 1999;39:1049–59.